ISSN: 2456-9348
Vol (03) _Issue (05) Impact Factor: 4.520

iJETRM
International Journal of Engineering Technology Research & Management

NUMERICAL STUDY OF FLOW FIELD ON THE COMBINED BLADE OF SAVONIUS WIND TURBINES

Arifin Sanusi
Department of Mechanical Engineering, Nusa Cendana University, Jalan Adi Sucipto, Kupang, 85001, Indonesia,
arifin_undana@yahoo.com

ABSTRACT
This research intended to improve the Savonius wind turbine performance by modifying its blade construction. Modification made in this research is to combine a conventional blade as the convex side and an elliptical blade as the concave side into a combined blade. This paper aimed to numerically analyze the flow pattern around the rotor of both the combined and conventional blades as well as the effects of changes in the Reynolds number on the turbine performance. A numerical study was carried out through computational fluid dynamics (CFD) using Ansys_Fluent 14.5. The numerical results of the coefficient of power (Cp) and coefficient of torque (Ct) were verified through the experimental results. Both of them showed an increased performance of the combined blade of the Savonius wind turbine. The combined blade has jet overlap and flow patterns which are greater than the conventional blade. Vortex and recirculation flow at the end of the conventional blade is smaller than that on the combined blade.

KEYWORDS:
Wind Turbine; Combined blade; CFD; Flow patterns

INTRODUCTION

The Savonius wind turbine is a vertical axis wind turbine (VAWT) as an alternative energy generation for renewable energy is able to operate despite in low wind speeds flowing from all directions; it has the simple construction and does not require a high tower. However, the efficiency of the Savonius wind turbine is apparently low compared with other turbine types (Zhou and Rempfer, 2013). Additional equipment on the turbine such as curtain and obstacle shielding in the returning blade may improve the performance of the turbines. Installation of the curtain can generate maximum power coefficient of 38% (Altan and Atılgan, 2010) and the installation of obstacle 25.8% (Mohamed et al., 2011). The use of deflector plate can increase the coefficient of power (Cp) up to 50% compared to the condition without deflector plate (Golecha et al., 2011). Likewise, the use of the guide box tunnel on a three-blade Savonius turbine can also increase the Cp to 50% compared to without guide box tunnel (Irabu and Roy, 2007). The developed three turbine cluster has an average power coefficient up to 34% higher than that of an isolated turbine (Shaheen et al., 2015). However, the addition of extra equipment may change the Savonius wind turbines to become more complex.

In order to achieve high power coefficient, the design should be positioned properly. Hence, it is necessary to study effective positioning of small scale wind turbines (Tummala et al., 2016). Therefore, the researchers develop the other methods to increase the performance of the Savonius wind turbine. The performance of Savonius turbine is influenced by the flow parameters and blade geometry (Akwa et al., 2012). Different geometry may give different results. Several modifications on the blade rotor have been carried out by researchers so that it develops into a helical blade (Kamoji et al., 2009a), twisted blade (Saha and Rajkumar, 2006), and elliptical blade (Kacprzak et al., 2013). The use of overlap and the value of the Reynolds number may affect the performance of Savonius turbine. The maximum coefficient of power increased with the increasing of Reynolds number (Kamoji et al., 2009b).

A research on a novel vertical axis wind turbine revealed that the shape of the rotor blade on the inside (concave side) and the outside (convex side) should become the focus of development to increase the torque generated by the rotor, making it more competitive with existing turbine designs (McTavish et al., 2012). Therefore, the existing blade models require continuous modifications to obtain better flow patterns in order to improve the turbine's performance. Turbine rotor with an elliptical blade has a more advanced overlapping flow so that it can produce greater thrust on the returning blade, but the structure of the stagnation point on the convex side is also larger, cause a decreasing of positive torque. Vice versa, the conventional blades generate thrust on the concave

iJETRM
International Journal of Engineering Technology Research & Management

side which is smaller than the elliptical models, but its convex side is better to reduce the size of stagnation point which causes of the negative torque.
The results of flow visualization on the Savonius rotor identified six main flow patterns that occur in the rotor blade which affect the operational characteristics of the turbine (Nakajima et al., 2008). The three types of the flows that contribute to the improved performance are attached flow, dragging flow and overlap flow, while the flows that have the degrading effect on the performance are stagnation flow and vortex flows on advancing and returning blade. Based on the flow pattern that occurs in the conventional and elliptical blades, there should be the combination of the blades to produce the supportive flow patterns to obtain better performance. The combined blade is made from a combination of the conventional blade as the convex side and elliptical blade the concave side. Analysis was conducted on the pattern of fluid flow in a rotor blade combined with changes in Reynolds number through computational fluid dynamics (CFD) using Ansys_fluent_14.5 Software.

OBJECTIVES

Design Rotor Blade

Turbine rotors which became the objects of analysis were combined blade and conventional blades. Dimensions and size of the combined blade were referred to the dimension and size of the conventional and elliptical blade in the study by Kacprzak et al. (Kacprzak et al., 2013) as shown in Figure 1.

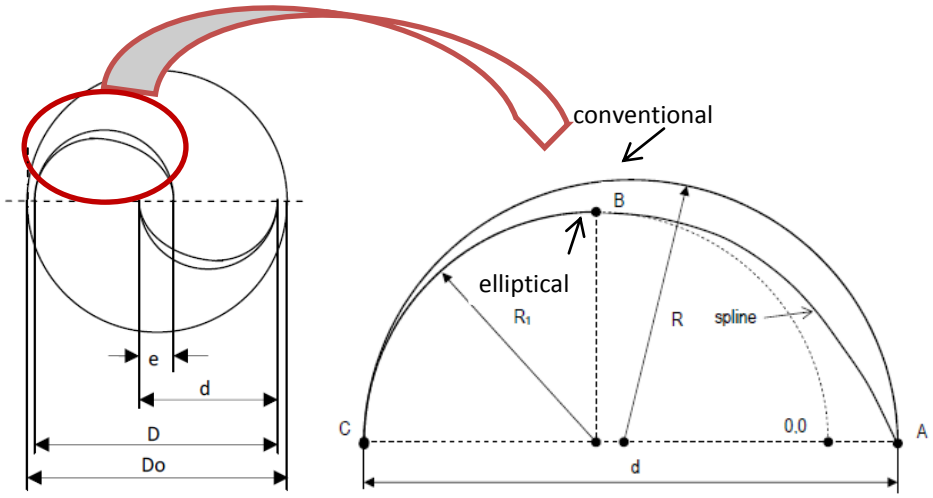

Fig. 1. Dimensions and configuration of the combined blade

Elliptical blade as the concave side was curved line connecting the coordinate points A (15 mm; 0), B (-50 mm; 50 mm), C (-100 mm; 0), where the line connecting points A and B were spline and connecting points B and C were the lines of a quarter circle with radius of R1 = 50 mm. Conventional blade model as the convex side was semicircular with the radius of R = 57.5 mm. End plate used to support blade rotor and the addition of end plates on a Savonius turbine can greatly increase the maximum average power of coefficient (Akwa et al., 2012). The use of both upper and lower end plates significantly increases the power coefficient by 36% compared with no end plates (Jeon et al., 2015). From those points would form the combined blade rotor with the diameter (D) = 200 mm, aspect ratio (H/D) = 1.0, diameter ratio of the end plate (Do/D) = 1.1, overlap ratio (e/D) = 0.15, chord diameter (d) = 115 mm (see Fig. 1).

METHODOLOGY

Numerical Simulation

iJETRM
International Journal of Engineering Technology Research & Management

Blade model was made by using modular design and fluent simulation of software Ansys Release 14.5. The simulations were developed from finite volume method (FVM) in which domain simulation was divided by the finite number of volume controls. The computational domain for simulation as shown in Figure 2 below:

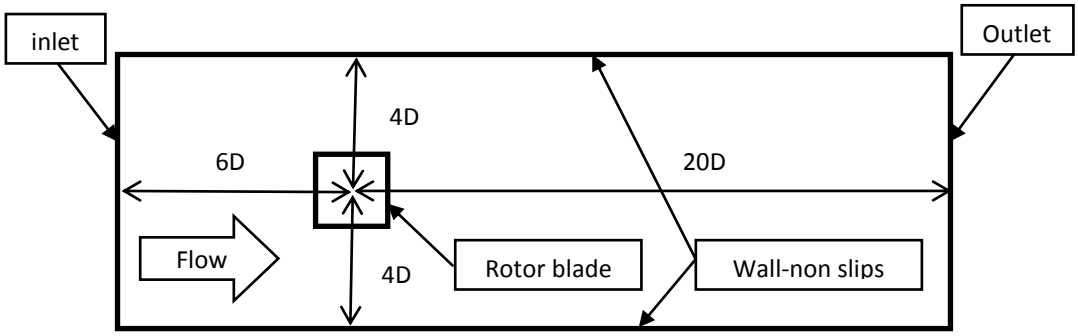

Fig. 2. Geometrical characteristics and boundary conditions of the computational domain

Simulations were carried out through sliding mesh method given with initial value through the simulation of multiple reference frames at TSR 0.1 to TSR 1.3. The time step referred to the rotation was 1 degree. The main difficulty dealing with actual geometry was the attainment of appropriate mesh. This study used triangular cells. Test independency grid each were carried out on the combined blade with the size of mesh-1= 40,000 cells, mesh-2 =80,000 cells and mesh-3=130,000 cells at TSR 0.8 and mesh-2 showed fairly accurate value in the analysis (Sanusi et al., 2017), the grids with approximately 80,000 and 120,000 elements gave substantially the same results. Considering the time economy in the simulation, the grid with 80,000 elements (Mao and Tian, 2015). The picture following shows combined blade and meshing used in the analysis in this paper (see Fig.3)

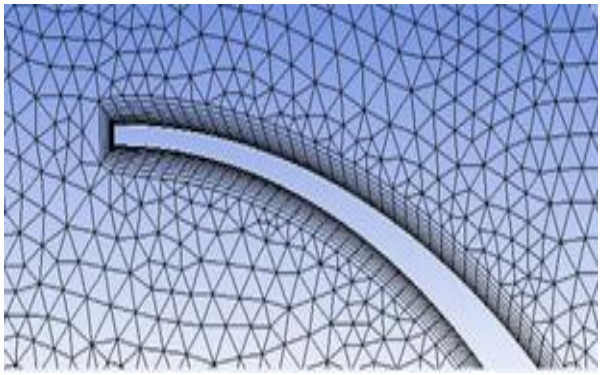

Fig. 3. Mesh combined blade (mesh-2=80.000 cells)

Based on the results of the grid test for the combined blade on TSR 0.8, the use of mesh-2 = 80,000 cells provided accurate results in the further analysis of both blade models. The average torque (TA) for each tip speed ratio (TSR) was analyzed to generate the value of the coefficient of torque (Ct) and coefficient of power (Cp) using Eq. (7) and Eq. (8).

The analysis focused on the effects in the area of rotor testing with two-dimensional simulation. The conservative or divergence form of the system of equations which governs the time-dependent two-dimensional fluid flow of an incompressible Newtonian fluid. In the following differential form of the governing equation are provided according to the computational model and their corresponding approximation as follows:

the conservation of mass equation or continuity equation is given by

$$\frac{\partial \rho}{\partial t} + \frac{\partial (\rho u)}{\partial x} + \frac{\partial (\rho v)}{\partial y} = 0 \qquad (1)$$

the conservation of momentum equation is given by

iJETRM
International Journal of Engineering Technology Research & Management

Momentum – x

$$\rho \frac{Du}{Dt} = \frac{\partial(-p+\tau_{xx})}{\partial x} + \frac{\partial \tau_{yx}}{\partial y} + S_{Mx} \quad (2a)$$

Momentum – y

$$\rho \frac{Dv}{Dt} = \frac{\partial \tau_{xy}}{\partial x} + \frac{\partial(-p+\tau_{yy})}{\partial y} + S_{My} \quad (2b)$$

The k-ε realizable model is substantially better than the standard k-ε model for many applications (Zhou and Rempfer, 2013). So that in this simulation, transport equation for the k-ε realizable model was used as follows:

$$\frac{\partial(\rho k)}{\partial t} + \frac{\partial(\rho k \mu_i)}{\partial x_i} = \frac{\partial\left[\left(\mu+\frac{\mu_t}{\sigma_k}\right)\left(\frac{\partial k}{\partial x_j}\right)\right]}{\partial x_j} + P_k + P_b - \rho\varepsilon - Y_M + S_k \quad (3)$$

$$\frac{\partial(\rho \varepsilon)}{\partial t} + \frac{\partial(\rho \epsilon \mu_i)}{\partial x_i} = \frac{\partial\left[\left(\mu+\frac{\mu_t}{\sigma_\epsilon}\right)\left(\frac{\partial \epsilon}{\partial x_j}\right)\right]}{\partial x_j} + \rho C_1 S_\epsilon - \rho C_2 \frac{\epsilon^2}{k+\sqrt{v\epsilon}} + C_{1\epsilon}\frac{\epsilon}{k} C_{3\epsilon} G_b + S_\epsilon \quad (4)$$

The turbulence viscosity was determined by: $\mu_t = \rho C_\mu \frac{k^2}{\varepsilon}$ (5)

Through dynamic studies allow analyzing the behavior of the rotors in relation to the velocity, pressure, and the vortices around the blade. The data input flows from left to right of wind velocity v = 5,999 m/s, the rotor rotation n = 459 rpm so that the value of tip speed ratio (TSR) gained is 0.8, which is the value that generally determines the highest value performance for Savonius wind turbine (Kacprzak et al., 2013).
Tip speed ratio is the ratio between the velocity at the tip of the blade and the wind velocity determined through the following equation:

$$TSR = \frac{\omega.R}{V} \quad (6)$$

The value coefficient of torque (Ct) and coefficient of power (Cp) use the following equation:

$$C_t = \frac{2T_A}{\rho_a A_T V^2 R} \quad (7)$$

$$C_p = C_t.TSR \quad (8)$$

In terms of the combined blade, it was simulated by the different inputs velocity, namely v=4 m/s, v=5,999 m/s and v=9 m/s to analyze the influence of the Reynolds number on the value of the same tip speed ratio (TSR = 0.8). The downstream pressure on the output 1 atm absolute, the density of the fluid ρ = 1.225 kg/m3, the fluid dynamic viscosity μ = 1.7895 x105 N.s/m2. The variations of air density were ignored and not treated as incompressible using a symmetric flow, so that the flow of vertical may be neglected. The criterion for convergence in the analysis of flow is 10-3 and 30 iterations per time step. The simulation is carried out for 30000-time steps in order to have a number of complete rotations

RESULTS AND DISCUSSION

The results of the simulation in the form of static pressure distribution and velocity apparently seem to show the different pattern of flow around the rotors against both blade models. The same input velocity and dimensions

produced different flow patterns. This shows that the shape of the blade significantly affects the flow patterns. Fig. 4 shows the distribution of static pressure that occurs in the rotor blade, where the combined blade shows that the static pressure in front of the concave side of the advancing blade was bigger than the conventional blade model. The pressure on the concave side of the blade was the main source of flow in generating thrust to the blade rotor of the turbine. The pressure on the concave side of the returning blade is influenced by the overlap on the rotor. The increased pressure on the concave side of the returning blade contributes to increasing the positive torque to the turbine. The use the elliptical model on the concave side of the combined blade can cause pressure on the concave side of the returning blade, so as to contribute positively to the increase of the torque. The pressure on the convex side of the advancing blade the conventional blade was considered low pressure at both tips, while on the convex side of the combined blade there was a sizable stagnation point structure on the returning blade [Fig. 4a]. The pressure on the convex side of the combined blade showed low pressure that develops away from the advancing blade, but on the convex side of the returning blade, the pressure was likely to be distributed evenly to the tip of the blade [Fig. 4b]. The contribution of low pressure on the convex side of the advancing blade plays the major role in improving the performance of the turbine (Zhou and Rempfer, 2013). Modification blade by integrated different concave and convex shapes (combined blade) make the static pressure of the convex side of the advancing blade becomes more centralized and reduces the stagnation point structures on the convex side of the returning blade.

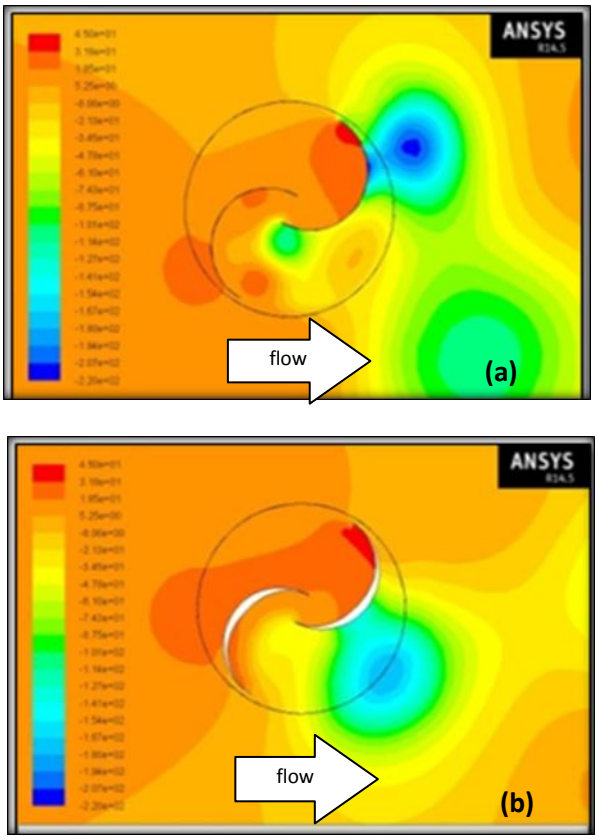

Fig. 4. Contour of static pressure: a) conventional blade, b) combined blade on TSR 0.8

iJETRM
International Journal of Engineering Technology Research & Management

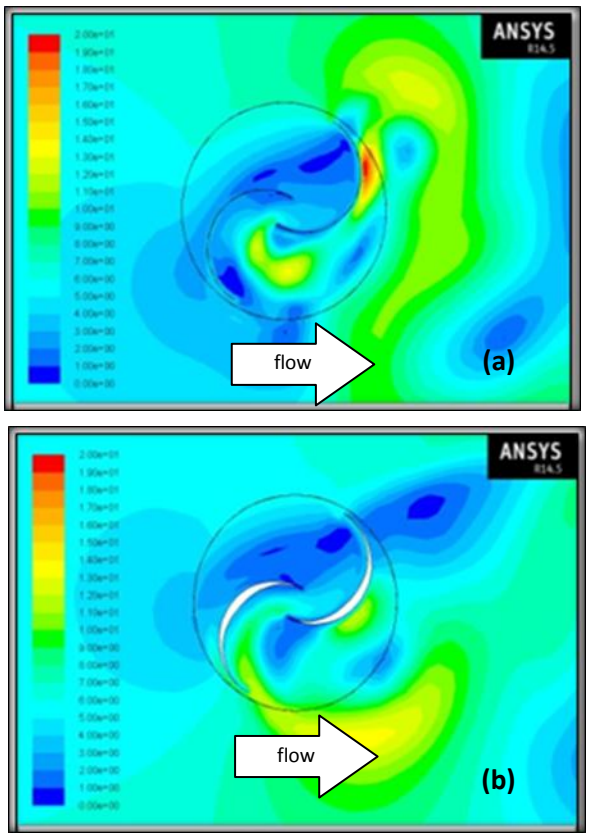

Fig. 5. Contour of velocity: a) conventional blade, b) combined blade on TSR 0.8

Figure 5 shows the contour of the velocity of the conventional blade and combined blade on the concave side of the returning blade which was likely high. For the combined blade, it was shown that the flow pattern was away from the rotor than the conventional blade, making it less influential to the flow on the convex side of the advancing blade and having the more positive role in giving the torque. The increased from the overlap effect of the jet which gives the flow to press the concave side of the back blade which produces positive results on increased torque on the turbine rotor. At the outer tip of the advancing blade, the recirculating flow seemed quite prominent in the conventional blade. The flow recirculation of the blade tip may cause the decreased performance of the turbine rotor (Nakajima et al., 2008). Vortices on the convex side of the advancing blade rotating clockwise can increase the strength of the suction pressure and lead to a decrease in torque (Zhou and Rempfer, 2013). Based on this, the fluid flowing behind the blade rotor greatly affects the performance of the turbine including shear forces. The flow of the convex side of the advancing blade and flow of overlap causes vortex at the tip of the advancing blade. Conventional blade (Fig. 5a) has a large vortex near the tip of the blade, while the combined blade was likely to grow out away from the rotor. The flow structure near the overlap was very complicated and influenced by the flow of the concave side of the advancing blade and Coanda-like flow along the concave side of the returning blade and the presence of flow circulation in the central rotor. The Coanda-like flow as the vortices flow in the overlap area of Savonius turbines migrates from the edge of the advancing blade to the concave side of the returning blade. The Coanda effect is the tendency of a fluid flow to adhere to a curved surface due to local pressure reduction by the acceleration of a fluid around a surface (De et al., 2017).

The results of the analysis of numerical data of all blade rotors have obtained the coefficient of torque (Ct) and coefficient of power (Cp). The experimental study has been done with a prototype of the same dimensions (Sanusi et al., 2016), the value with the same trend although the numerical value was lower than the experimental results as shown in Fig.6 and Fig.7. In the experimental case, more possibilities of errors can be found because of equipment and human imperfection (Morshed et al., 2013). Increased blockage ratio caused

iJETRM
International Journal of Engineering Technology Research & Management

increased pressure on the wall of the wind tunnel due to a narrowing of the testing areas so that the speed of the flow is actually increased and produce higher power coefficient (Cp) (Ross and Altman, 2011).

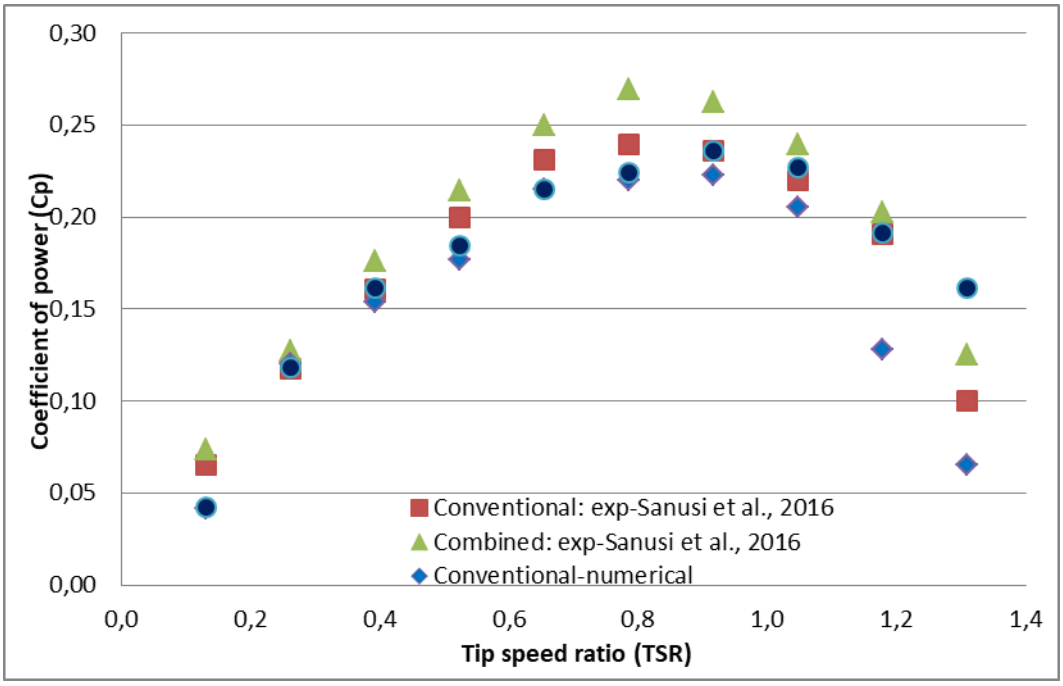

Fig. 6. Comparison coefficient of power (C_p) vs TSR for conventional and combined blades

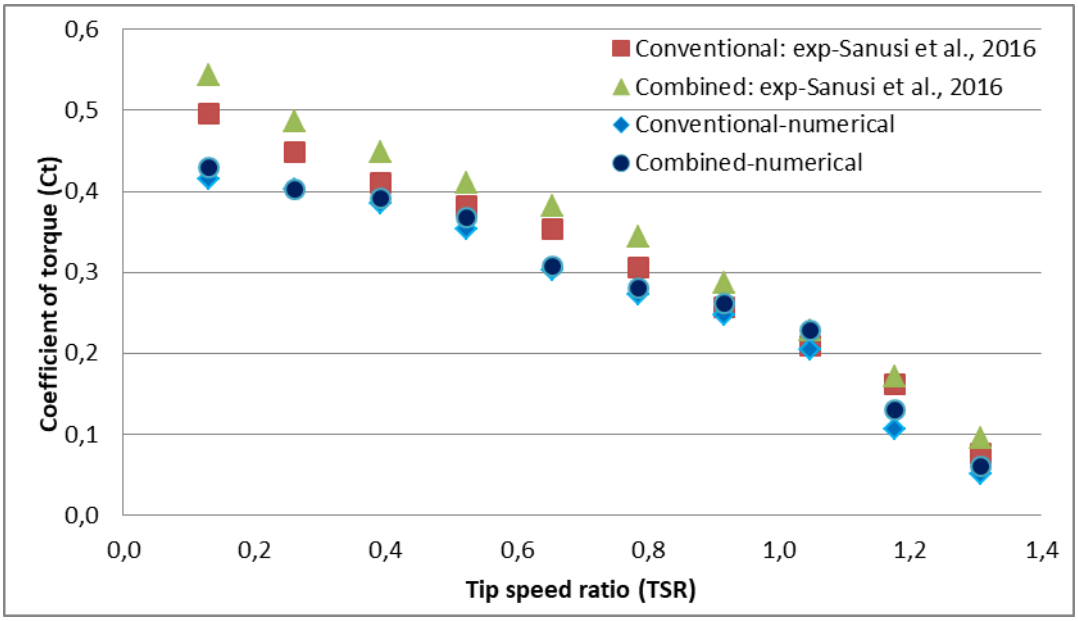

Fig. 7. Comparison coefficient of torque (C_t) vs TSR for conventional and combined blades

Figure 6 shows the value of the coefficient of power (Cp) based on the results of numerical and experimental analyses of the conventional blade and combined blade. It was widely perceived that the combined blade has a higher coefficient of power (Cp) than the conventional blade. The results of the numerical analysis showed the differences in the value of the coefficient of power (Cp) which was quite large at TSR > 0.8. The numerical

results of coefficient of power (Cp) on the conventional blade was in accordance with the simulation [9]. Figure 7 is the comparison coefficient of torque (Ct) of the conventional blade and the combined blade shown through numerical analysis and experimental results. The coefficient of torque (Ct) of the combined blade showed improvement from the conventional blade, despite the fact that the percentage was relatively small

ACKNOWLEDGEMENT

The author would like to thank the Director of Research and Community Service of the Ministry of Research, Technology and Higher Education of the Republic of Indonesia for financial support of National Strategic Research with the title Utilized Wind Turbines with Combined Blade as Alternative Energy Source.

CONCLUSION

The results of numerical studies of the conventional blade rotor and combined blade are shown with the flow pattern that occurs as stated in the following:

- Modification blade (combined blade) make the static pressure of the convex side of the advancing blade becomes more centralized and reduces the stagnation point structures on the convex side of the returning blade.
- The flow patterns on the combined blade cause the increase of jet overlap, and the decreasing vortex on the convex side compared with the conventional blade.
- The coefficient of power (Cp) and coefficient of torque (Ct) increase using combined blade.

REFERENCES

[1] Akwa, J.V., Vielmo, H.A., Petry, A.P., A review on the performance of Savonius wind turbines. Renewable and Sustainable Energy Reviews 16, pp. 3054–3064, 2012. https://doi.org/10.1016/j.rser.2012.02.056

[2] Altan, B.D., Atılgan, M., The use of a curtain design to increase the performance level of a Savonius wind rotors. Renewable Energy 35, pp. 821–829, 2010. https://doi.org/10.1016/j.renene.2009.08.025

[3] De, L., Vieira, R., Isoldi, L., Oliveira, R., Dos, S., Dos, S., Numerical analysis of a turbulent flow with Coanda effect in hydrodynamics profiles. FME Transaction 45, pp. 412–420, 2017. https://doi.org/10.5937/fmet1703412L

[4] El-Askary, W.A., Nasef, M.H., AbdEL-hamid, A.A., Gad, H.E., Harvesting wind energy for improving performance of Savonius rotor. Journal of Wind Engineering and Industrial Aerodynamics 139, pp. 8–15, 2015. https://doi.org/10.1016/j.jweia.2015.01.003

[5] Golecha, K., Eldho, T.I., Prabhu, S.V., Influence of the deflector plate on the performance of modified Savonius water turbine. Applied Energy 88, pp. 3207–3217, 2011. https://doi.org/10.1016/j.apenergy.2011.03.025

[6] Irabu, K., Roy, J.N., Characteristics of wind power on Savonius rotor using a guide-box tunnel. Experimental Thermal and Fluid Science 32, pp. 580–586, 2007. https://doi.org/10.1016/j.expthermflusci.2007.06.008

[7] Jeon, K.S., Jeong, J.I., Pan, J.-K., Ryu, K.-W., Effects of end plates with various shapes and sizes on helical Savonius wind turbines. Renewable Energy 79, pp. 167–176, 2015. https://doi.org/10.1016/j.renene.2014.11.035

[8] Kacprzak, K., Liskiewicz, G., Sobczak, K., Numerical investigation of conventional and modified Savonius wind turbines. Renewable Energy 60, pp. 578–585, 2013. https://doi.org/10.1016/j.renene.2013.06.009

[9] Kamoji, M.A., Kedare, S.B., Prabhu, S.V., Performance tests on helical Savonius rotors. Renewable Energy 34, pp. 521–529, 2009a. https://doi.org/10.1016/j.renene.2008.06.002

[10] Kamoji, M.A., Kedare, S.B., Prabhu, S.V., Experimental investigations on single stage modified Savonius rotor. Applied Energy 86, pp. 1064–1073, 2009b. https://doi.org/10.1016/j.apenergy.2008.09.019

[11] Mao, Z., Tian, W., Effect of the blade arc angle on the performance of a Savonius wind turbine. Advances in Mechanical Engineering 7, pp. 1-10, 2015. https://doi.org/10.1177/1687814015584247

[12] McTavish, S., Feszty, D., Sankar, T., Steady and rotating computational fluid dynamics simulations of a novel vertical axis wind turbine for small-scale power generation. Renewable Energy 41, pp. 171–179, 2012. https://doi.org/10.1016/j.renene.2011.10.018
[13] Mohamed, M.H., Janiga, G., Pap, E., Thévenin, D., Optimal blade shape of a modified Savonius turbine using an obstacle shielding the returning blade. Energy Conversion and Management 52, pp. 236–242, 2011. https://doi.org/10.1016/j.enconman.2010.06.070
[14] Morshed, K.N., Rahman, M., Molina, G., Ahmed, M., Wind tunnel testing and numerical simulation on aerodynamic performance of a three-bladed Savonius wind turbine. International Journal of Energy and Environmental Engineering 4, pp. 1-14, 2013.
[15] Nakajima, M., Shouichiro, I.I.O., Ikeda, T., Performance of Savonius rotor for environmentally friendly hydraulic turbine. Journal of Fluid Science and Technology 3, pp. 420–429, 2008.
[16] Ross, I., Altman, A., Wind tunnel blockage corrections: Review and application to Savonius vertical-axis wind turbines. Journal of Wind Engineering and Industrial Aerodynamics 99, pp. 523–538, 2011. https://doi.org/10.1016/j.jweia.2011.02.002
[17] Saha, U.K., Rajkumar, M.J., On the performance analysis of Savonius rotor with twisted blades. Renewable Energy 31, pp. 1776–1788, 2006. https://doi.org/10.1016/j.renene.2005.08.030
[18] Sanusi, A., Soeparman, S., Wahyudi, S., Yuliati, L., Performance Analysis of a Combined Blade Savonius Wind Turbines. International Journal of Fluid Machinery and Systems 10, pp. 54–62. 2017.
[19] Sanusi, A., Soeparman, S., Wahyudi, S., Yuliati, L., Experimental Study of Combined Blade Savonius Wind Turbine. International Journal of Renewable Energy Research (IJRER) 6, pp. 614–619, 2016.
[20] Shaheen, M., El-Sayed, M., Abdallah, S., Numerical study of two-bucket Savonius wind turbine cluster. Journal of Wind Engineering and Industrial Aerodynamics 137, pp. 78–89, 2015. https://doi.org/10.1016/j.jweia.2014.12.002
[21] Tummala, A., Velamati, R.K., Sinha, D.K., Indraja, V., Krishna, V.H., A review on small scale wind turbines. Renewable and Sustainable Energy Reviews 56, pp. 1351–1371, 2016. https://doi.org/10.1016/j.rser.2015.12.027
[22] Zhou, T., Rempfer, D., Numerical study of detailed flow field and performance of Savonius wind turbines. Renewable Energy 51, pp. 373–381, 2013. https://doi.org/10.1016/j.renene.2012.09.046